ASSESSMENT OF THE CRACK SYSTEM ORIENTATIONS OF A CERAMIC MATRIX COMPOSITE UNDER OFF-AXIS TENSILE LOADING

Stéphane Baste and Christophe Aristégui

Université Bordeaux 1
Laboratoire de Mécanique Physique, CNRS URA 867
351 Cours de la Libération 33405 Talence cedex, France

INTRODUCTION

To emphasize the anisotropy induced by damage on a ceramic matrix composite subjected to a tensile solicitation at 30° from one of the fiber directions, the changes of all the stiffness tensor components are determined from wave speed measurements of obliquely incident ultrasonic bulk waves. Using the additive form of the stiffness tensor of the damaged material, the crack orientation is determined from the damage tensor, i.e., the part relative to the loss of stiffness caused by the microcracks. The search for the principal frame of this tensor from wave speed measurements allows the assessment of the microcrack orientation.

Moreover, by defining the damage as the change of the elasticity tensor [1], no preliminary knowledge of the microstructure is required. Comparison between the experimental measurements of the damage carried out without *a priori* crack geometry and theoretical predictions of the changes in elasticity coefficients deduced from an ideal representation [2], allows identification of the approximate orientation of the microcracking.

The measurements were performed on a woven 2D C-C-SiC obtained from SEP (Société Européenne de Propulsion, France). Identification of the global elastic properties from wave speed measurements has already shown both the initial quasi-hexagonal symmetry of this composite and the load-induced rotation of the elasticity principal frame [3].

ANISOTROPIC DAMAGE

The purpose of the continuum damage concept, introduced first by Kachanov in 1958, is to describe, in terms of continuum mechanics, internal structure change that occurs in certain materials under stress. It is now commonly recognized that the Young modulus

Review of Progress in Quantitative Nondestructive Evaluation, Vol. 17
Edited by D.O. Thompson and D.E. Chimenti,, Plenum Press, New York, 1998

variation is the correct measure of damage which is experimentally realizable [4]. The three-dimensional generalization leads us naturally to define damage as a change of the elasticity tensor [1]. The elasticity tensor **C** of the damaged material can be written in an additive form [5], where:

$$\omega = \mathbf{C}_0 - \mathbf{C} \tag{1}$$

is the damage tensor due to the microcracks and $\mathbf{C}_0$ is the stiffness tensor of the uncracked material. This form of the effective elasticity tensor is in line with the analytical expressions of the elasticity constants of an elastic solid with distributed cracks, that were obtained from micromechanical approaches.

The components of the tensor ω can be measured using an immersion ultrasonic method, they have a clearly identifiable physical meaning and form a finite set of data. No particular symmetry class must be postulated for both the initial material and the cracked one [6]. It is able to describe fully anisotropic behavior.

UNDER LOAD ULTRASONIC DEVICE

The under load characterization device described in Figure 1, allows one to measure the phase velocities of obliquely incident ultrasonic waves propagating in the material under stress [7]. Ultrasonic experiments are performed in pulsed through transmission. By inverting the Christoffel equation [8], the stiffness tensor (C_{IJ}) can be determined from wave speed measurements in a suitable set of incident planes [9, 6]. During the tensile test, the total longitudinal strain along the loading direction is measured using an extensometer.

The dimensions, geometry and orientation of the used specimens are displayed in Figure 2. The density is close to 2.06 g/cm^3. For each sample, a coordinate system R=($\mathbf{x}_1$, $\mathbf{x}_2$, $\mathbf{x}_3$) for ultrasonic measurements is chosen in such a way that axis $\mathbf{x}_1$ corresponds to the normal to the plate, Figure 1.

The quasi-isotropy of the cloths plane ($\mathbf{x}_2$, $\mathbf{x}_3$) which has been already emphasized [3] explains naturally the similarity of the elastic response, i.e., at the beginning of the solicitation, Figure 2.

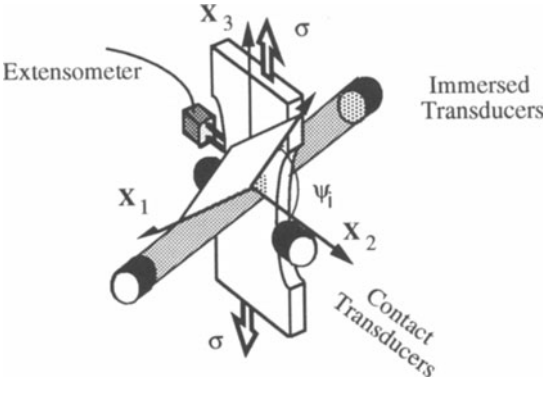

Figure 1. Ultrasonic device used to investigate the stress-induced development of the damage of the 2D C-C-SiC composite. All incident planes ($\mathbf{x}_1$, Ψ_i) are defined by an azimuthal angle Ψ_i.

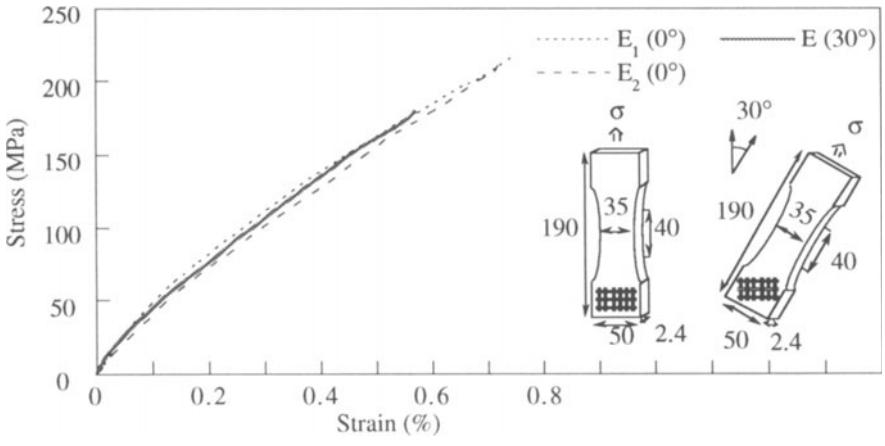

Figure 2. Stress-strain curves measured for the samples $E_1(0°)$, $E_2(0°)$ and $E(30°)$ of 2D C-C-SiC composite. Schematic representation of the specimens orientation and dimensions (given in millimeters).

However, this composite does not exhibit an elastic behavior. A non-linearity, very similar for each sample, appears from the onset of loading. So, the record of the total longitudinal strain does not emphasize an appreciable difference of the damage process during these tensile tests, either in a principal direction or in a non-principal direction. Only the failure stress and the failure strain vary according to the direction of solicitation.

By using the ultrasonic device, a study [10] on the behavior of this composite under on-axis loading, samples $E_1(0°)$ and $E_2(0°)$, has shown that the cracks grow preferentially in the plane transverse to the loading direction, then is deflected in mode II at the fiber-matrix interface. The degradation process preserves the elasticity principal frame associated with the fibers, but destroys the balance of the carbon cloths. The initial tetragonal elastic symmetry becomes increasingly orthorhombic [10].

TENSILE LOADING IN A NON-PRINCIPAL DIRECTION

The changes of the thirteen components of the damage tensor (ω_{IJ}), Equation (1), calculated from the experimentally measured stiffness tensors (C_{IJ}) for the sample E(30°), are plotted in Figure 3 as a function of the applied tensile stress. The ultrasonic data are reported in this volume [3].

No elastic-linear behavior domain is observed; the increase of the damage moduli appears from the onset of the loading and continues near linearly until the maximum stress. The increase of damage along the tensile axis $\mathbf{x}_3$ is very important and occurs from the first stress levels. The instantaneous matrix microcracking oriented normally to the tensile stress appears from the loading onset and affects similarly the moduli ω_{44} and ω_{13}. The brittlness of the C-SiC matrix does not induce the premature failure of the composite. The fibrous reinforcement stops and deviates the matrix microcracking. The experimental changes of the stiffnesses ω_{11}, ω_{22}, ω_{66} and ω_{12} point out the generation of others cracking modes [11].

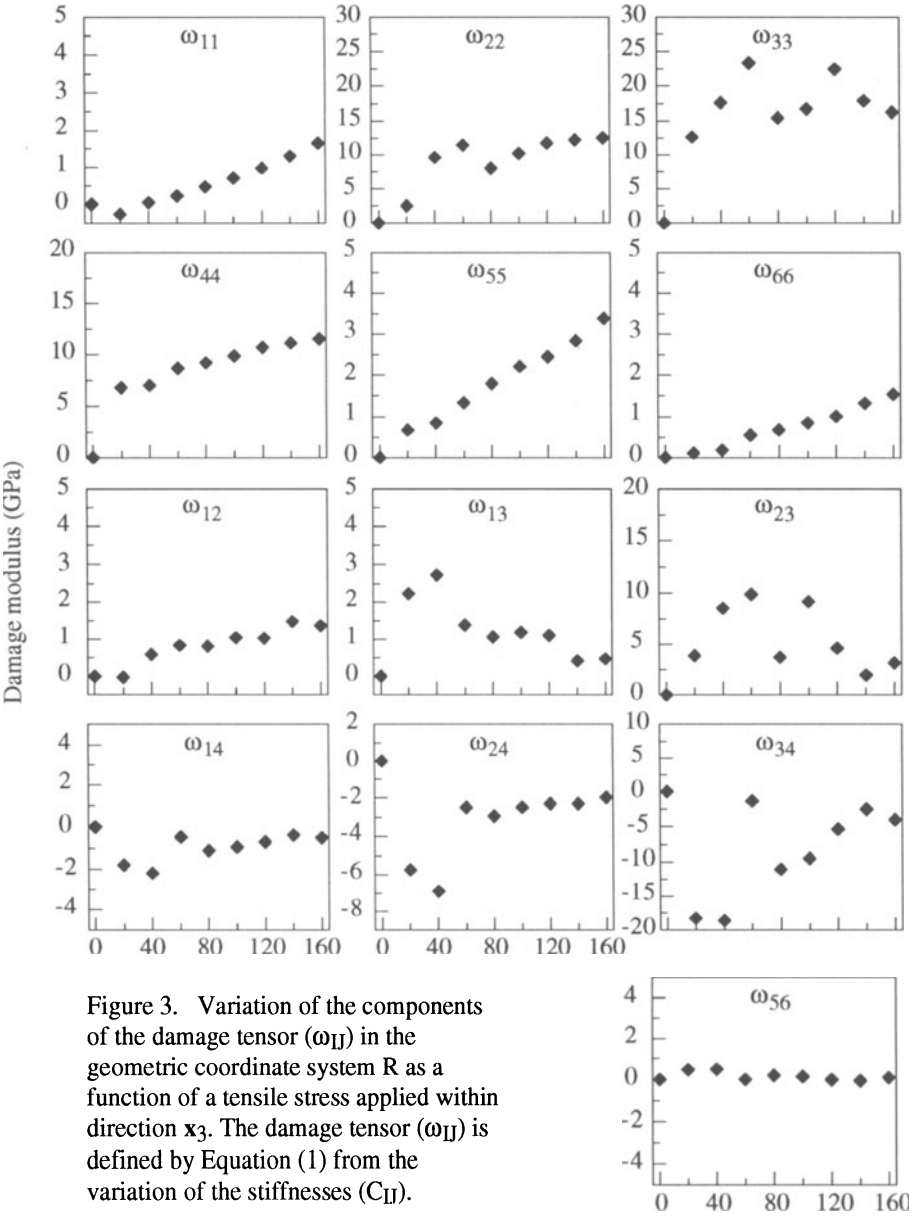

Figure 3. Variation of the components of the damage tensor (ω_{IJ}) in the geometric coordinate system R as a function of a tensile stress applied within direction $\mathbf{x}_3$. The damage tensor (ω_{IJ}) is defined by Equation (1) from the variation of the stiffnesses (C_{IJ}).

Orientation of the Crack Systems

Due to the rigidness of the ceramic matrix, the orientation of the fibers is *a priori* preserved during the 30° off-axis loading, and consequently, the frame $R^f=(\mathbf{x}_1, \mathbf{x}_2^f, \mathbf{x}_3^f)$ associated with the fibrous reinforcement is assumed to be fixed. This frame is chosen in such a way that the two base vectors $\mathbf{x}_2^f$ and $\mathbf{x}_3^f$ are aligned with the fiber direction. The angle (ϕ^f) between the axes $\mathbf{x}_2$ and $\mathbf{x}_2^f$ is equal to 30°.

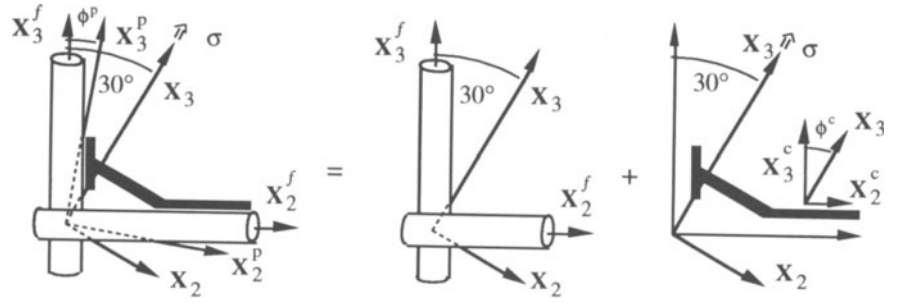

Figure 4. Description of the microcracked material by the superposition between the uncracked material and the microcracks.

The additive form of the stiffness tensor of the damaged material, Equation (1), allows one to describe the elastic properties of the microcracked material by the effect of the microcracks on the undamaged material, Figure 4. Three principal frames take place in this decomposition: the elasticity principal coordinate system of the damaged material R^p which turns during the solicitation [3], the elasticity frame of the uncracked material R^f which coincides with the fixed frame associated with the fibers, and the frame related to the orientation of the crack systems. The R^p rotation [3] is due to the non-superposition of these two last coordinate systems.

Using the general expression of the effective elasticity moduli of a microcracked material, it is interesting to study the orientation of the crack systems through the form of the damage tensor (ω_{IJ}), Equation (1). A transverse matrix microcracking normal to the $\mathbf{x}_3$-loading direction, Figure 5, fundamental mechanism of degradation of ceramic matrix composites, affects indeed only five damage moduli, ω_{33}, ω_{44}, ω_{55}, ω_{13} and ω_{23} [11]. On the other hand, the superposition of three mutually orthogonal slit crack systems, Figure 6, influences the whole set of the components of the following tensor [12]:

$$\begin{bmatrix} \omega_{11} & \omega_{12} & \omega_{13} & & & \\ & \omega_{22} & \omega_{23} & & 0 & \\ & & \omega_{33} & & & \\ & & & \omega_{44} & & \\ & \text{Sym.} & & & \omega_{55} & \\ & & & & & \omega_{66} \end{bmatrix}. \tag{3}$$

Where the damage tensor (ω_{IJ}) takes the form (3), there exists probably three mutually orthogonal crack system which coincide with the base vectors of the frame in which the tensor is expressed. This principal frame of the damage tensor (ω_{IJ}) is therefore related to the orientation of the microcracks.

From the thirteen components of the damage tensor (ω_{IJ}), Figure 3, the "microcracking" principal frame is searched. Only the crack systems lying in the plane ($\mathbf{x}_2$, $\mathbf{x}_3$) can be considered [10]. Let $R^c=(\mathbf{x}_1, \mathbf{x}_2^c, \mathbf{x}_3^c)$ be a frame whose base vector $\mathbf{x}_2^c$ is aligned with a crack system. In the coordinate system R^c, the tensor (ω_{IJ}) takes the form (3). The determination of the angle ϕ^c relative to the rotation about the $\mathbf{x}_1$ axis and relating the base vectors $\mathbf{x}_2$ and $\mathbf{x}_2^c$, locates the frame R^c with respect to the geometric coordinate system R, and consequently, the orientation of a crack system comparative to the cloths plane ($\mathbf{x}_2$, $\mathbf{x}_3$).

Let $R_\phi=(\mathbf{x}_1, \mathbf{x}_2^\phi, \mathbf{x}_3^\phi)$ be the current frame obtained from a ϕ-degree rotation of R about the $\mathbf{x}_1$ axis. The equivalent damage tensor (ω_{IJ}) (ϕ) in the frame R_ϕ is obtained from

the tensor (ω_{IJ}) using the fourth-rank tensor rotation laws. Assuming that the current frame R_ϕ coincides with a "microcracking" principal coordinate system, the damage tensor $(\omega_{IJ})(\phi)$ takes the form (3) and is noted $(\omega_{IJ})_\phi$. If R_ϕ is the searched principal frame, the damage tensor in the geometric frame R, equivalent to $(\omega_{IJ})_\phi$, is identical to the damage tensor (ω_{IJ}), Figure 3. The angle ϕ^c, locating the crack systems parallel to the directions $\mathbf{x}_2^c$ and/or $\mathbf{x}_3^c$, is determined by solving:

$$\phi^c = \min_{\phi \in [-\pi/2;\, \pi/2]} \sum_{\substack{I=1 \text{ to } 6 \\ J=1 \text{ to } 6}} \left(\omega_{IJ} - \omega_{IJ}^{\phi}\right)^2 . \tag{4}$$

Solving the problem (4) shows the existence of two "microcracking" principal frames, R_1^c and R_2^c, Figure 7. These coordinate systems, defined by the angles $\phi_1^c=0°$ and $\phi_2^c=30°$ respectively, are fixed during the test and are different from the moving elasticity principal coordinate system R^p [3]. The poor quality of the experimental measurements at 60 MPa explains the identification of a single angle ϕ^c.

Due to the superposition of two differently oriented crack systems, the two identified frames R_1^c and R_2^c are strongly, but not strictly, principal frames for the damage tensor (ω_{IJ}). The angles ϕ_1^c and ϕ_2^c are not zeros but minima of the functional to be minimized in Equation (4). The orientation of the microcracks could then be identified by breaking down the global tensor (ω_{IJ}) into parts $(\omega_{IJ})^c$ associated with each crack system.

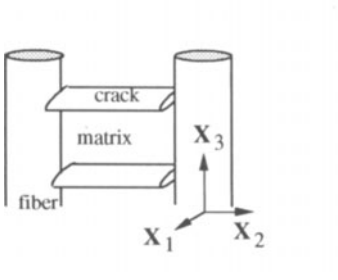

Figure 5. Schematic geometry of transverse matrix microcracks by a slit crack system.

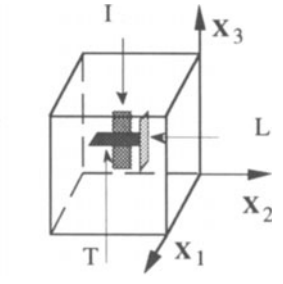

Figure 6. Modeling of the various damage modes by three orthogonal penny-shaped crack systems [12].

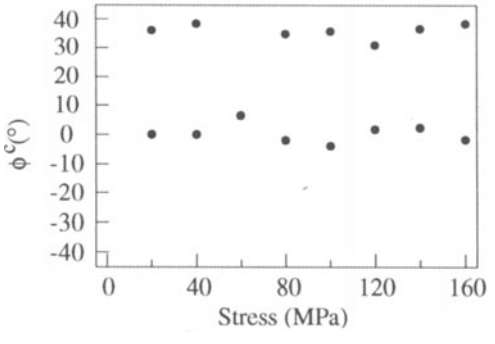

Figure 7. Orientation of the crack systems with respect to the geometric frame R during the tensile test. The angle ϕ^c relates the axis $\mathbf{x}_2$ and these crack systems. The identified values have been obtained by solving the problem (4).

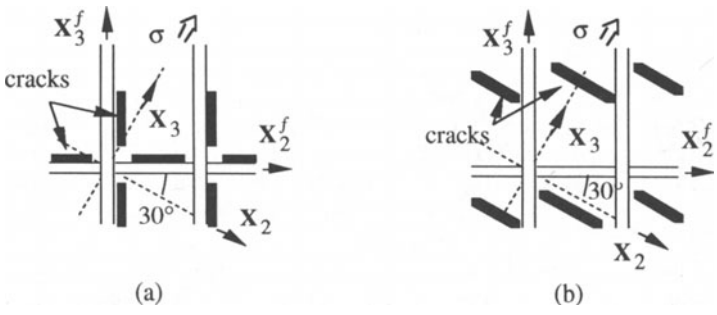

Figure 8. Damage modes taking place during the 30° off-axis solicitation: (a) matrix transverse microcracking normal to the loading direction, (b) microcracking extends along the fibers. The frame $R^f=(\mathbf{x}_1, \mathbf{x}_2^f, \mathbf{x}_3^f)$ associated with the fibers is fixed during the loading.

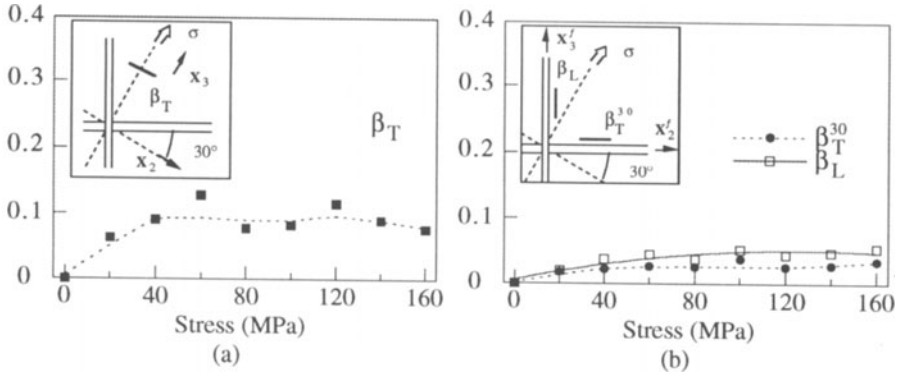

Figure 9. Change of the crack-density parameters during a 30° tensile loading: (a) transverse matrix microcracking, (■) β_T in the frame R; (b) microcracking governed by the fiber directions, (•) β_T^{30} and ( ) β_L in the frame R^f.

Each of the base vectors $\mathbf{x}_2^c$ and $\mathbf{x}_3^c$ of the "microcracking" principal frame R^c can correspond to a crack system. In R_1^c, two directions; $\phi^c=0°$ and $\phi^c=90°$, can coincide with a cracking orientation. The observed increase of the damage modulus ω_{33}, clearly more important than the one of ω_{22}, Figure 3, shows the predominance of the transverse matrix microcracks ($\phi^c=0°$), Figure 8(a). The existence of each of the two possible orientations related to R_2^c, $\phi^c=30°$ and $\phi^c=120°$, Figure 8(b), must be still studied.

The geometry of cracks, created by this 30° off-axis solicitation, is certainly complex. The crack orientation does not coincide with the elasticity principal axes of the composite. To assess accurately the crack density parameters of the three identified crack systems, Figure 8, the analytical predictions of the effective elastic properties of an orthorhombic solid containing tilted cracks must be used. This case having never been treated to our knowledge, the simple micromechanical model (5) is used to show the analysis which can be carried out from the global elastic properties measurements (ω_{IJ}), Figure 3.

To describe these experimental variations, revealing a three-dimensional damage, three different systems of slit cracks (schematically represented in Figure 6) can be introduced. Assuming the effects of the various crack systems are additive and independent, the compliance tensor **S** of the cracked material becomes [2, 12]:

$$\mathbf{S} = \mathbf{S}_0 + \frac{\pi\,\beta_T}{4}\,\Lambda^T + \frac{\pi\,\beta_L}{4}\,\Lambda^L + \frac{\pi\,\beta_I}{4}\,\Lambda^I, \qquad (5)$$

where Λ^T, Λ^L and Λ^I are the interaction tensors of the crack systems "T", "L" and "I". Through their respective crack-density parameter β_T, β_I and β_L, the "T" damage mode can describe the transverse matrix microcracks oriented normally to the tensile stress, the "I" damage mode may be regarded mainly as bundle-matrix debonding and interply delamination whereas the "L" damage mode incorporates bundle-matrix and fiber-matrix debonding. The identification of the three crack densities β_T, β_L and β_I only requires the knowledge of the initial compliance tensor $\mathbf{S}_0$ and the experimental measurements of the damage-induced change of the compliances S_{33}, S_{22} and S_{11}, respectively. A damage mode with a given orientation can therefore be defined by a single parameter: the crack density.

A first estimation of the crack density parameters associated with the three crack systems reported in Figure 8 may therefore be performed by considering that the geometric coordinate system R ($\approx R_1^c$) and the frame R^f associated with the fibers ($\approx R_2^c$) are successively elasticity principal frames [10], Figure 9. Two fiber-matrix debonding modes defined by ϕ^c=30° and ϕ^c=120° are emphasized, Figure 8(b). The three crack systems extend from the load beginning, then tend to saturate from an applied stress of 40 MPa. The transverse matrix microcracking constitutes the basic damage mechanism. The variations β_L and β_T^{30} are representative of the mode II deflection of the matrix cracks along the axes $\mathbf{x}_3^f$ and $\mathbf{x}_2^f$ respectively. The failure mechanisms favor the generation of microcracks perpendicular to the tensile loading direction stress when the distance between fibers is large enough.

CONCLUSION

The assessment of the crack orientation, from the wave speed measurements, has shown the existence of three microcracking modes in the cloths plane: the matrix cracking normal to the applied load and the deviation in mode II of these matrix microcracks along the fibers oriented at 30° and 120° with respect to the loading direction. Then, by comparing the measured stiffness change carried out and the effective elasticity coefficient predictions of body containing cracks, both the three crack-density parameters; β_T, β_L and β_T^{30}, and the associated crack orientations, have been determined. Moreover, the difference between the damage mechanisms relative to the on-symmetry and to the off-symmetry axis tensile loading, emphasized by using the immersion ultrasonic method, has not been detected by the classical longitudinal strain measurement technique.

REFERENCES

1. S. Baste and B. Audoin, Eur. J. Mech. A/Solids 10, 587 (1991).
2. N. Laws, Philosophical magazine 36, 367 (1977).
3. C. Aristégui and S. Baste, in *Review of Progress in QNDE*, Vol. 17, eds D. O. Thompson and D. E. Chimenti (Plenum press, New York, 1997), these proceedings.
4. D. Krajcinovic, Mech. Mater. 8, 117 (1989).
5. M. Ortiz, Mech. Mater. 4, 67 (1985).
6. C. Aristégui and S. Baste, J. Acoust. Soc. Am. 101, 813 (1997).
7. B. Audoin, "Évaluation ultrasonore de l'endommagement anisotrope d'un composite à matrice fragile", Ph. D. University Bordeaux I (1991).
8. B. A. Auld, *Acoustic Fields and Waves in solids* (Wiley-Interscience, New York, 1973).
9. S. I. Rokhlin and W. Wang, J. Acoust. Soc. Am. 91, 3303 (1992).
10. S. Baste and C. Aristégui, submitted to Mech. Mater.
11. S. Baste and R. El Bouazzaoui, J. Composites Matérials 30, 282 (1996).
12. R. El Bouazzaoui, S. Baste and G. Camus, C. Sci. and Tech. 56, 1373 (1996).